Chemistry–A European Journal
Research Article
doi.org/10.1002/chem.202400856
Chemistry Europe
European Chemical Societies Publishing
www.chemeurj.org

VIP *Very Important Paper*

Ferromagnetically Coupled Chromium(III) Dimer Shows Luminescence and Sensitizes Photon Upconversion

Simon Trippmacher,[a] Serhiy Demeshko,[b] Alessandro Prescimone,[c] Franc Meyer,[b] Oliver S. Wenger,*[a] and Cui Wang*[a, d]

There has been much progress on mononuclear chromium(III) complexes featuring luminescence and photoredox activity, but dinuclear chromium(III) complexes have remained underexplored in these contexts until now. We identified a tridentate chelate ligand able to accommodate both meridional and facial coordination of chromium(III), to either access a mono- or a dinuclear chromium(III) complex depending on reaction conditions. This chelate ligand causes tetragonally distorted primary coordination spheres around chromium(III) in both complexes, entailing comparatively short excited-state lifetimes in the range of 400 to 800 ns in solution at room temperature and making photoluminescence essentially oxygen insensitive. The two chromium(III) ions in the dimer experience ferromagnetic exchange interactions that result in a high spin ($S=3$) ground state with a coupling constant of $+9.3\ cm^{-1}$. Photoinduced energy transfer from the luminescent ferromagnetically coupled dimer to an anthracene derivative results in sensitized triplet-triplet annihilation upconversion. Based on these proof-of-principle studies, dinuclear chromium(III) complexes seem attractive for the development of fundamentally new types of photophysics and photochemistry enabled by magnetic exchange interactions.

Introduction

Recently, remarkable progress has been made with luminescent first-row transition metal complexes, based for example on vanadium,[1] chromium,[2] manganese,[3] iron,[4] nickel,[5] copper,[6] and zinc,[7] which provided important insights into molecular design principles and the application potential of photoactive 3d metal compounds.[8] These new types of photoactive metal complexes are promising alternatives to platinum group metal compounds, due to their photophysical and photochemical properties,[2k,8a,c] which allow their investigation in sensing,[9] lighting,[6c,10] photon upconversion,[7b,11] and photocatalysis.[2k,6e,12]

Important progress has been made in recent years with mononuclear luminescent Cr^{III} complexes with tridentate polypyridyl ligands, which lead to large ligand field splittings, in many cases due to the strongly σ-donating and π-accepting character and the almost perfectly octahedral geometry (with N-Cr^{III}-N bite angles approaching 90°) reached in many of the recently reported new complexes.[2a–d,g,i,13] These Cr^{III} complexes show spin-flip doublet excited states ($^2T_1/^2E$), often with high photoluminescence quantum yields and lifetimes up to the millisecond-scale in solution at room temperature,[2a–d,f,g,13] and some of these Cr^{III} complexes exhibit high excited state redox potentials.[12c,e,14] These photophysical and photochemical properties make photoactive Cr^{III} complexes attractive for applications relying on energy- and electron-transfer processes,[8d,11b,f,12c–e,14–15] for example energy transfer- or photoredox catalysis.

The long-lived spin-flip excited states of many mononuclear Cr^{III} complexes permit efficient oxygen quenching via a Dexter-type energy transfer mechanism.[2a,16] A recent study showed that charge-transfer based deactivation can also be a factor in the oxygen quenching.[17] Effective oxygen quenching makes luminescent Cr^{III} complexes promising oxygen sensors[9a] and photosensitizers for generating singlet oxygen ($^1O_2$) in photocatalysis[18] and photodynamic therapy.[15,19] However, the oxygen-sensitivity restricts the application potential of the Cr^{III} complexes in lighting or in energy transfer processes with other substrates under ambient conditions. Therefore, different strategies have been developed to suppress the oxygen sensitivity of luminescent Cr^{III} complexes, such as introducing bulky substituents to the ligand,[20] using sterically demanding counter anions,[9e] or encapsulating the Cr^{III} complexes into oxygen shielding matrices.[9e,21]

Polynuclear Cr^{III} complexes have so far been mostly explored in the context of magnetic phenomena,[22] but aside from selected early studies[23] they have received limited attention yet in contemporary optical spectroscopic studies. Dinuclear Cr^{III} complexes exhibiting room temperature luminescence while preserving ferromagnetic exchange interactions seem attractive

[a] S. Trippmacher, Prof. Dr. O. S. Wenger, Prof. Dr. C. Wang
Department of Chemistry, University of Basel, St. Johanns-Ring 19, 4056 Basel, Switzerland
E-mail: oliver.wenger@unibas.ch
cui.wang@uni-osnabrueck.de
[b] Dr. S. Demeshko, Prof. Dr. F. Meyer
Institute of Inorganic Chemistry, University of Göttingen, Tammannstraße 4, 37077 Göttingen, Germany
[c] Dr. A. Prescimone
Department of Chemistry, BPR 1096, University of Basel, Mattenstrasse 24a, 4058 Basel, Switzerland
[d] Prof. Dr. C. Wang
Department of Biology and Chemistry, Osnabrück University, Barbarastraße 7, 49076 Osnabrück, Germany

Supporting information for this article is available on the WWW under https://doi.org/10.1002/chem.202400856

for developing luminescent single-molecule magnets, which until now rely mostly on lanthanide ions.[24] Numerous hydroxo- and oxo-bridged dinuclear Cr^{III} complexes have been developed to explore the magnetic exchange interactions, and in most cases, the two Cr^{III} centers are antiferromagnetically coupled in their electronic ground states.[22,25] There have been only few examples of dinuclear Cr^{III} complexes with ferromagnetic coupling,[26] but there exist strategies for obtaining ferromagnetically coupled Cr^{III} compounds.[27] Recently explored dinuclear Cr^{III} complexes have a $Cr^{III}(\mu\text{-OR})_2(\mu_{1,3}\text{-carboxylato})Cr^{III}$core structure, exhibiting ferromagnetic coupling constants up to $+8\ cm^{-1}$.[27] Replacement of the bis-μ-alkoxido with bis-μ-thiolato bridges increased the ferromagnetic exchange coupling constant to $J = +(24–34)\ cm^{-1}$ for the dinuclear Cr^{III} complexes $[Cr_2L_2(\mu\text{-SR})_2(\mu\text{-}O_2CR)]^{3+}$ with an amino-thiophenolato ligand (Figure 1).[28] Attempts were made to make dinuclear Cr^{III} complexes photoluminescent, while maintaining the ferromagnetic coupling, but only few examples are known and their photoluminescence at room temperature was very weak.[28]

The tridentate chelate ligand dNinp (2,6-di(*N*-7-azaindol-1-yl)pyridine) is a structural analogue to dqp (2,6-di(quinolin-8-yl)pyridine) and ddpd (*N*,*N*′-dimethyl-*N*,*N*′-dipyridin-2-ylpyridine-2,6-diamine), all of which fulfill the structural requirements to form six-membered chelating rings and large N-M-N bite angles near 90° with the coordinated metal center (Figure 1), such as previously observed with Ru^{II}.[29] Coordination of ddpd or dqp to Cr^{III} ion led to mononuclear near-infrared (NIR) emitters with favorable photophysical and photochemical properties as noted above,[2a,b,d,i] while luminescent Cr^{III} complexes with the dNinp ligand do not seem to have been reported yet.

In this study, we coordinated dNinp to Cr^{III} ion, giving mono- and dinuclear Cr^{III} complexes that can be synthesized in a controlled manner. Magnetic measurements of the hydroxo- and carboxylato-bridged dinuclear Cr^{III} complex (Figure 1, bottom right) indicated ferromagnetic exchange interactions between the two Cr^{III} centers in their electronic ground state with a coupling constant of $J = +9.3\ cm^{-1}$. Both the new mono- and dinuclear Cr^{III} complexes exhibit photoluminescence in solution at room temperature with time constants of several hundreds of nanoseconds. Spectroscopic investigations indicate that the luminescence of these Cr^{III} complexes is insensitive to oxygen, contrasting the behavior of the vast majority of recently explored luminescent Cr^{III} complexes. These excited state properties permit the dinuclear ferromagnetically coupled Cr^{III} complex to be used as a photosensitizer for triplet-triplet annihilation upconversion.

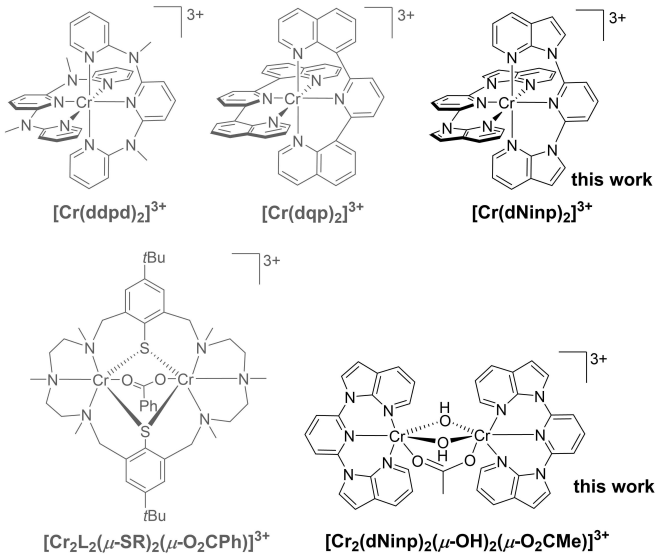

Figure 1. Molecular structures of mononuclear luminescent $[Cr(ddpd)_2]^{3+}$ (ddpd = *N*,*N*′-dimethyl-*N*,*N*′-dipyridin-2-ylpyridine-2,6-diamine),[2d] $[Cr(ddpd)_2]^{3+}$ (dqp = 2,6-di(quinolin-8-yl)pyridine),[2a] and $[Cr(dNinp)_2]^{3+}$ (dNinp = 2,6-di(*N*-7-azaindol-1-yl)pyridine) (this work), as well as dinuclear luminescent Cr^{III} complexes $[Cr_2L_2(\mu\text{-SR})_2(\mu\text{-}O_2CPh)]^{3+}$[28] and $[Cr_2dNinp_2(\mu\text{-OH})_2(\mu\text{-}O_2CMe)]^{3+}$ (this work).

Results and Discussion

Synthesis and characterization: The ligand dNinp was synthesized by Ullman-type coupling of 2,6-dibromopyridine with 7-azaindole by adapting a literature procedure,[30] giving nearly quantitative product yield (SI, section 2.1). Acetonitrile as the reaction solvent allowed the formed ligand to precipitate, which simplifies the product purification by filtration. The mono- and the dinuclear Cr^{III} complexes were then synthesized in a controlled manner by either starting from a Cr(II) or a Cr(III) precursor as illustrated in Figure 2. Coordination with dNinp using more reactive chromium(II)[2a] occurred in the presence of silver triflate, and subsequent oxidation with oxygen from air in the presence of potassium triflate gave the desired mononuclear $[Cr(dNinp)_2]^{3+}$ complex as a triflate salt with a complexation yield of 73% (Figure 2, top right). Replacing silver triflate and potassium triflate with their corresponding hexafluorophosphate salts gave the PF_6-salt of the $[Cr(dNinp)_2]^{3+}$ complex. Vapor diffusion of diethyl ether into an acetonitrile solution of the mononuclear complex gave single crystals suitable for X-ray diffraction analysis.

For the preparation of $[Cr_2(dNinp)_2(\mu\text{-OH})_2(\mu\text{-}O_2CMe)]^{3+}$, chromium(III) chloride tetrahydrofuran complex was used as the metal precursor (Figure 2b, SI, section 2.3).[2g,31] Using a multistep microwave synthesis, which is a well-known procedure for the preparation of heteroleptic Cr^{III} complexes,[31] a dinuclear Cr^{III} complex (Cr_2-OTf) bridged by two hydroxo-ligands and one carboxylato-ligand was obtained, in which each Cr^{III} center is furthermore coordinated by one dNinp ligand (Figure 2b). The bridging acetate and hydroxides are likely formed from acetonitrile and water traces under the harsh reaction conditions.[32] Counter anion exchange with potassium hexafluorophosphate gave the corresponding PF_6-salt of the dinuclear Cr^{III} complex (Cr_2-PF_6). Red needle-shaped single crystals suitable for X-ray diffraction analysis were obtained for both dinuclear salts. Mass spectrometry and elemental analysis confirmed the structures and the purity of the mono- and dinuclear Cr^{III} complexes.

X-ray diffractometric analysis: Single crystal analysis of $[Cr(dNinp)_2](PF_6)_3$ reveals a pseudo-octahedral CrN_6 coordination geometry of the cation $[Cr(dNinp)_2]^{3+}$ with the N-Cr^{III}-N bite angles close to 90° and 180° (Table 1, Figure 3a). These angles are favorable to induce a large ligand-field splitting, similar to the

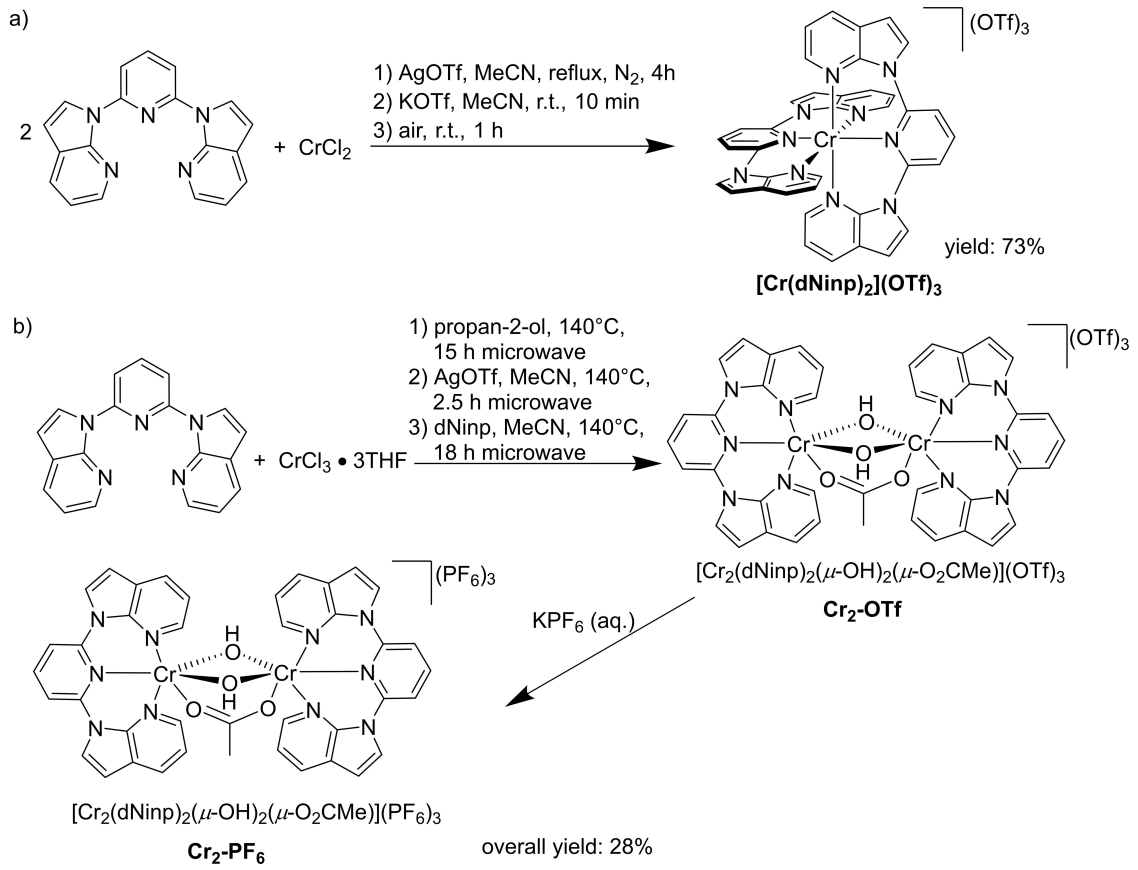

Figure 2. Synthetic procedures for preparing a) mononuclear $[Cr(dNinp)_2]^{3+}$ complex and b) dinuclear $[Cr_2(dNinp)_2(\mu\text{-}OH)_2(\mu\text{-}O_2CMe)]^{3+}$ as the OTf-salt (Cr_2-OTf) and the PF_6-salt (Cr_2-PF_6).

Table 1. Pertinent crystal structure parameters of a few selected Cr^{III} complexes bearing tridendate polypyridine ligands: $[Cr(dqp)_2]^{3+}$,[2d] $[Cr(ddpd)_2]^{3+}$,[2a] and $[Cr(dNinp)_2](PF_6)_3$ (this work). N_L = lateral coordinating pyridine nitrogen atom, N_C = central coordinating pyridine nitrogen atom.

Complex	*$[Cr(dqp)_2]^{3+}$ (ref. [2d])*	*$[Cr(ddpd)_2]^{3+}$ (ref. [2a])*	*$[Cr(dNinp)_2]^{3+}$ (this work)*
N_L-Cr-N_C angle/°	87.6(1)/88.1(1)	85.7(3)/ 86.7(3)	87.5(1)/89.4(1)
N_C-Cr-N_C angle/°	179.6(1)	178.6 (0.3)	179.7(4)
N_L-Cr-N_L angle/°	175.8(1)	172.3(2)	176.7(1)
N_L-Cr length/ Å	2.037(3)/ 2.040(3)	2.028(6)/ 2.041(6)	2.029(1)/ 2.044(1)
N_C-Cr length/ Å	2.070(2)	2.054(7)	2.100(1)

that found for $[Cr(dqp)_2]^{3+}$[2d] and $[Cr(ddpd)_2]^{3+}$.[2a] The Cr^{III}-N_L distances are 2.029(1)/2.044(1) Å for the lateral pyridines and 2.100(1) Å for the central pyridine (Cr^{III}-N_C, Table 1, Figure 3a). Evidently, the CrN_6 coordination geometry is tetragonally elongated, similarly to what was previously found for the RuN_6 unit in $[Ru(dNinp)_2]^{2+}$.[29b] The dinuclear Cr^{III} complex crystallizes in a symmetrical butterfly-like structure with the two coordinated dNinp ligands spreading outwards (Figure 3b). The Cr^{III}-Cr^{III} distance of 2.948(2) Å points to the absence of a formal metal-metal bond.[33] Shorter lateral Cr^{III}-N_L distances (2.046–2.070 Å) than the central Cr^{III}-N_C distances (2.104–2.107 Å) are also found for the dinuclear Cr^{III} complex, which are all longer than the Cr^{III}-O bonds with the bridging hydroxo and carboxylato groups (1.940–1.960 Å, Table 2). The N_L-Cr^{III}-N_L bite angle of ~100° is much smaller than that for the mononuclear Cr^{III} complex (176.7(1)°), implying a facial coordination character for the dNinp ligand in the dinuclear compared to the mononuclear complex (Figure 3b, Table 2). For each Cr^{III} center in the dimer, coordination with one tridentate dNinp ligand and three O atoms from the two hydroxides and the acetate results in distorted pseudo-octahedral geometry. The Cr^{III}-O_H-Cr^{III} bridging angle of ~98° is similar to other dinuclear Cr^{III} complexes with the same bridging units,[27] but larger than the Cr^{III}-S-Cr^{III} angle of ~93° in the dimeric $[Cr_2L_2(\mu\text{-}SR)_2(\mu\text{-}O_2CPh)]^{3+}$ (Table 2).[28]

Magnetic properties: Polynuclear Cr^{III} complexes with ferromagnetic coupling between the octahedral metal centers are attractive compounds for developing new magnetic materials, because the $3d^3$ ion Cr^{III} usually possesses sizeable magnetic moments due to the half-filled t_{2g} orbital set.[34] Temperature-dependent magnetic susceptibility measurements were carried out for the dinuclear Cr_2-OTf (Fig. 4). Upon decreasing temperature, the magnetic susceptibility steadily increases to reach a maximum $\chi_M T$ value of 5.80 $cm^3 mol^{-1}$ K at $T = 12$ K, which drops to 5.27 $cm^3 mol^{-1}$ K at $T = 2$ K likely due to saturation effects. At

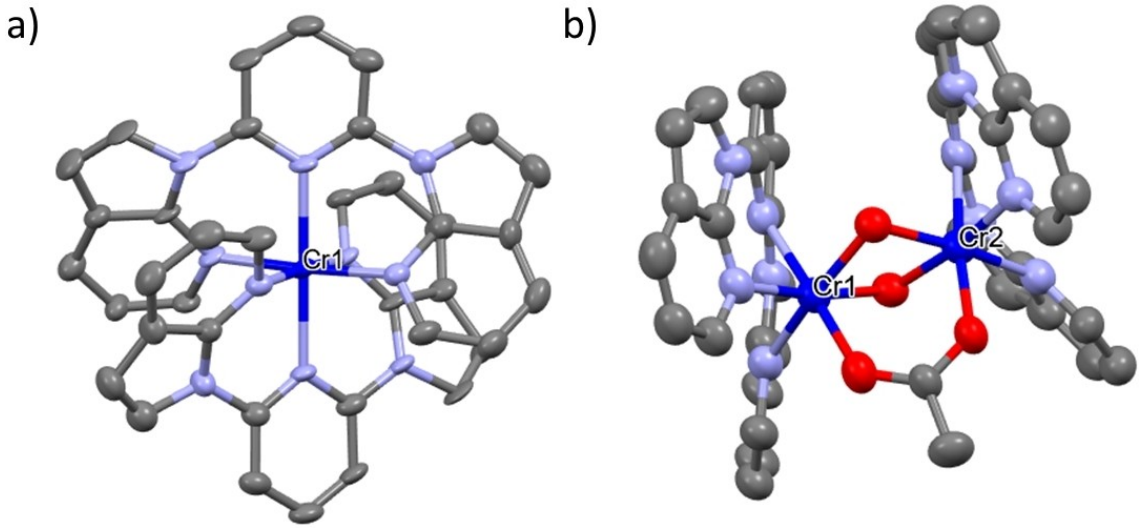

Figure 3. X-ray single crystal structures of a) the mononuclear $[Cr(dNinp)_2](PF_6)_3$ and b) the dinuclear $[Cr_2(dNinp)_2(\mu\text{-}OH)_2(\mu\text{-}O_2CMe)](PF_6)_3$. Hydrogen atoms, counter ions, and solvents are omitted. Color code: Cr = dark blue; N = blue; O = red; C = grey. Thermal ellipsoids drawn at 50% probability.

Table 2. Pertinent crystal structure parameters of the dinuclear Cr^{III} complexes $[Cr_2L_2(\mu\text{-}SR)_2(\mu\text{-}O_2CPh)]^{3+}$[28] and Cr_2-OTf as well as Cr_2-PF_6 (this work) with respect to one Cr^{III} center (Cr2). N_L = lateral coordinating pyridine nitrogen atom, N_C = central coordinating pyridine nitrogen atom, O_H = oxygen atom of the bridging hydroxide; O_C = oxygen atom of the bridging acetate.

Dinuclear Cr^{III} complex	*$[Cr_2L_2(\mu\text{-}SR)_2(\mu\text{-}O_2CPh)]^{3+}$[28]*	*Cr_2-OTf (this work)*	*Cr_2-PF_6 (this work)*
N_L-Cr2-N_C angle/°	–	86.5(2)/ 86.2(2)	85.2(3)/ 87.5(2)
N_L-Cr2-N_L angle/°	–	100.9(2)	99.7(3)
Nc-Cr2-O_C angle/°	–	174.2(2)	173.3(2)
N_L-Cr2-O_H angle/°	–	167.7(2)/ 170.3(2)	169.3(3)/ 169.5(3)
Cr1-O_H-Cr2 angle/°	92.16(4)/94.01(4) (Cr1-S-Cr2)	97.9(2)/ 97.8(2)	98.5(3)/ 98.1(3)
Cr1-Cr2 length/Å	3.545(1)	2.933(1)	2.948(2)
N_L-Cr2 length/Å	2.166(4)/2.213(4)	2.061(5)/ 2.070(8)	2.046(6)/ 2.067(8)
N_C-Cr2 length/Å	2.129(3)	2.107(5)	2.104(6)
O_H-Cr2 length/Å	2.434(1)/2.400(1) (S-Cr2)	1.940(4)/ 1.944(5)	1.944(5)/ 1.946(7)
O_C-Cr2 length/Å	1.954(3)	1.947(5)	1.960(6)

295 K, the $\chi_M T$ value of 4.00 is slightly higher than the expected value for two non-interacting ions with $S = 3/2$ and $g = 2.00$ (3.75 $cm^3 mol^{-1} K$). These features indicate a ferromagnetic exchange interaction between the two Cr^{III} centers to give rise to an $S_T = 3$ ground state. Magneto-structural studies found that dihydroxo-bridged dinuclear Cr^{III} complexes are typically antiferromagnetically coupled,[22,25,35] while the introduction of an additional carboxylato-bridge can lead to ferromagnetically coupled systems,[27] in agreement with our observations. Fitting to the spin Hamiltonian $\hat{H}$ (eq. 1) gives a coupling constant J of $+9.3$ cm^{-1}.

$$\hat{H} = -2J\hat{S}_1\hat{S}_2 + g\mu_B\vec{B}\left(\vec{S}_1 + \vec{S}_2\right) \quad (1)$$

where $\hat{S}_1$ and $\hat{S}_2$ stand for the electron spins of the two Cr^{III} ions, μ_B is the Bohr magneton, and B indicates the magnetic flux density. The resulting J value is large when compared to other ferromagnetically coupled dinuclear Cr^{III} complexes with dihydroxo- and carboxylato-bridges.[22,27] In comparison to the $[Cr_2L_2(\mu\text{-}SR)_2(\mu\text{-}O_2CPh)]^{3+}$ complex, which holds an exceptionally high J value of 34.8 cm^{-1} for ferromagnetically coupled Cr^{III} complexes,[28] the smaller J value for the present dinuclear Cr^{III} complex is likely attributable to the abovementioned larger Cr^{III}-O_H-Cr^{III} bridging angles according to systematic magneto-structural correlation studies.[27]

Photophysical Properties

The UV-vis absorption spectrum of $[Cr(dNinp)_2](OTf)_3$ shows an absorption band at 312 and a shoulder at 352 nm (Figure 5a), which are assigned to the typical ligand-based $\pi\rightarrow\pi^*$ and ligand-to-metal charge transfer (LMCT) transitions, respectively. Following earlier studies of $[Cr(tpy)_2]^{3+}$ and $[Cr(ddpd)_2]^{3+}$,[2a,36] the absorption band maximizing at 425 nm is attributed to the energetically lowest-lying spin-allowed transition from the $^4A_2$ ground state to the $^4T_2$ excited state. The molar extinction coefficient at this wavelength is unusually large for an MC transition in octahedral symmetry ($\varepsilon = 3250$ $M^{-1} cm^{-1}$), but the same observation has been previously made for $[Cr(ddpd)_2]^{3+}$.[37] Aside from the relaxation of the Laporte (parity) selection rule owing to the lack of an inversion center, the tail of an LMCT absorption band or the mixing with LMCT transitions could contribute to the comparatively high ε value at 425 nm.[2a] The

$^4A_2 \rightarrow {}^4T_2$ absorption band in $[Cr(dNinp)_2]^{3+}$ is found at very similar wavelength as in $[Cr(tpy)_2]^{3+}$ (422 nm)[36] and in $[Cr(ddpd)_2]^{3+}$ (435 nm),[2a] indicating a similarly strong ligand-field in all three complexes. A weak absorption shoulder observed in the spectrum of $[Cr(dNinp)_2](OTf)_3$ at ~620 nm is tentatively attributed to spin-forbidden $\pi \rightarrow {}^3\pi^*$ transitions (inset of Fig. 5a), as observed in $[Cr(dqp)_2]^{3+}$.[2d,38] The Laporte- and spin-forbidden $^4A_2 \rightarrow {}^2T_2/{}^2T_1/{}^2E$ transitions, which are typically below 5 $M^{-1}\,cm^{-1}$ in six-coordinate complexes possessing an inversion center,[39] could not be identified under the applied measurement conditions. Upon photoexcitation at 425 nm, spin-flip luminescence from the doublet excited states $^2T_1/{}^2E$ is observed at 730/770 nm (full width at half maximum (FWHM) = 370 cm^{-1} for the 770 nm emission). These two excited states are typically in thermal equilibrium (Figure 5a, Figure 5c, left).[8e] The $^2T_1/{}^2E$ emission wavelengths of $[Cr(dNinp)_2](OTf)_3$ are energetically near those of $[Cr(tpy)_2]^{3+}$ (770 nm)[36] and $[Cr(ddpd)_2]^{3+}$ (738/775 nm),[2a] but slightly longer than in $[Cr(dqp)_2]^{3+}$ (724/747 nm).[2d] The excitation spectrum monitoring the emission intensity at 770 nm (solid blue trace in Fig. 5a) follows the UV-vis absorption spectrum closely between 550 and 380 nm, in line with expectation. At shorter wavelengths, inner filter effects cause the excitation spectrum to deviate from the absorption spectrum, which is a common observation.

The dinuclear Cr^{III} complex shows an LMCT absorption band peaking at 347 nm, at a similar wavelength as in $[Cr(dNinp)_2]^{3+}$ (352 nm), while the lowest-lying MC absorption band in the dinuclear complex is shifted to ~500 nm (Figure 4b) and features a substantially lower molar extinction coefficient (ε = 148 $M^{-1}\,cm^{-1}$) than in the monomer complex (3250 $M^{-1}\,cm^{-1}$, see above). The lower energy of this MC transition likely results from the weaker ligand-field strength (10 Dq ~ 20000 cm^{-1}) in the dinuclear complex than in $[Cr(dNinp)_2]^{3+}$ (10 Dq ~ 23500 cm^{-1}), caused by the bridging hydroxides and the acetate as weak-field ligands, and perhaps additionally the more distorted octahedral geometry for the Cr^{III} ions in the dimer (see above). The ligand field parameters 10 Dq given here were determined directly from the lowest-energy UV-vis absorption band maxima, and they are seen as crude approximations of the true values, due to the partial overlap of the LMCT absorption tail with the MC absorption band, or even possible LMCT/MC mixing as noted above. For dinuclear Cr^{III} complexes, only one of the two metal ions is formally involved in the MC transitions,[40] thus the lowest-lying MC transition is referred to as $^4A_2{}^4A_2 \rightarrow {}^4T_2{}^4A_2$. The Laporte- and spin-forbidden $^4A_2{}^4A_2 \rightarrow {}^2T_1{}^4A_2/{}^2E{}^4A_2$ transitions were not detectable under our measuring conditions. The excitation spectrum monitoring the emission intensity at 728 nm (solid blue trace in Figure 5b) matches the UV-Vis absorption spectrum

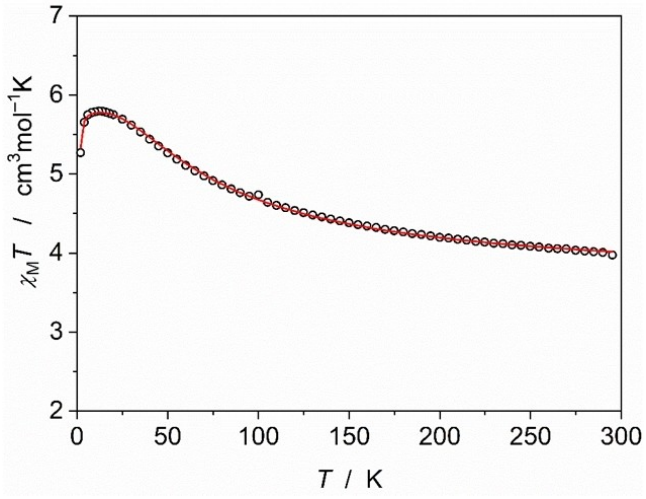

Figure 4. Variable-temperature magnetic susceptibility data for Cr_2-OTf. The red curve represents the best fit with the parameters: J = +9.3 cm^{-1} and $g_1 = g_2 = 1.97$.

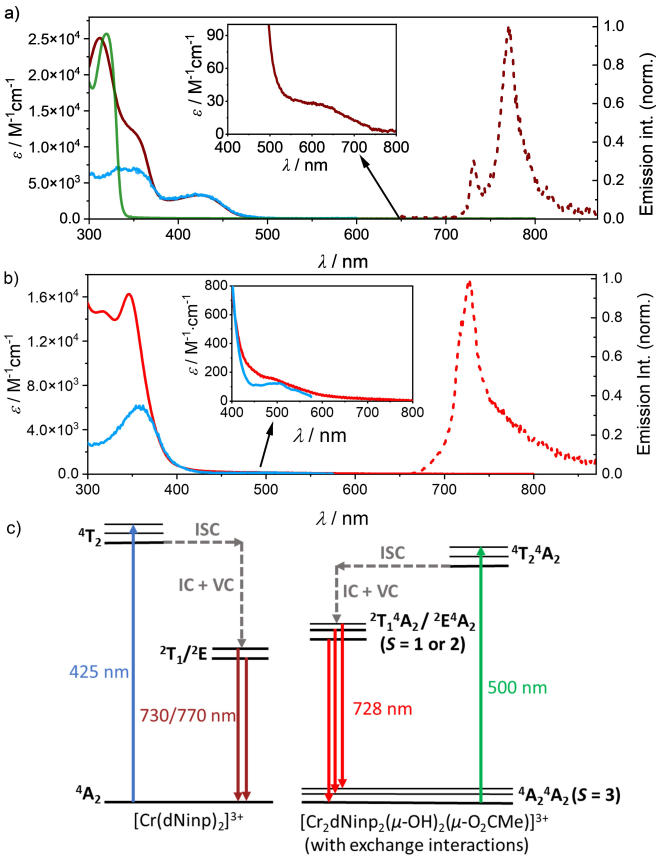

Figure 5. a) UV-vis absorption spectra of the dNinp ligand in dichloromethane (green solid trace) and $[Cr(dNinp)_2](OTf)_3$ in acetonitrile (dark red solid trace) at 20 °C, together with the excitation spectrum (emission detected at 770 nm) (bright blue solid trace) and normalized luminescence spectrum of $[Cr(dNinp)_2](OTf)_3$ in deaerated acetonitrile at 20 °C (excitation at 425 nm) (dotted dark red trace). Inset: UV-vis absorption spectrum of $[Cr(dNinp)_2](OTf)_3$ enlarged in the range from 400 to 800 nm. b) UV-vis absorption spectrum of Cr_2-PF_6 in acetonitrile (red solid trace) at 20 °C, together with the excitation spectrum (emission detected at 728 nm) (bright blue solid trace) and the normalized luminescence spectrum in deaerated acetonitrile at 20 °C (excitation at 350 nm) (dotted red trace). Inset: UV-vis absorption spectrum and excitation spectrum of Cr_2-PF_6 enlarged in the range from 400 to 800 nm. c) Simplified energy level diagram of the mononuclear $[Cr(dNinp)_2]^{3+}$ (left) and the dinuclear $[Cr_2(dNinp)_2(\mu\text{-}OH)_2(\mu\text{-}O_2CMe)]^{3+}$ complexes with exchange interactions (right). *S* stands for the spin states resulting from exchange interactions in the dimeric complex, here only shown for the emissive excited states $^2T_1{}^4A_2/{}^2E{}^4A_2$ and the $^4A_2{}^4A_2$ ground state. ISC: intersystem crossing, IC: internal conversion, VC: vibrational cooling.

within experimental accuracy, and inner filter effects can account for their discrepancy at shorter wavelengths.

The luminescence spectra of Cr_2-PF_6 and Cr_2-OTf in acetonitrile contain a band centered at 728 nm at room temperature (Figure 5b), arising from the radiative decay from the $^2T_1{}^4A_2/^2E^4A_2$ excited states to the $^4A_2{}^4A_2$ ground state (Figure 5c, right).[28] The luminescence band (FWHM = 550 cm^{-1}) is broader than for $[Cr(dNinp)_2]^{3+}$, likely because more convoluted excited and ground state manifolds are involved in the emission transition due to the magnetic exchange interactions (Figure 5c), in line with previous observations in $[Cr_2L_2(\mu\text{-}SR)_2(\mu\text{-}O_2CPh)]^{3+}$[28] and other dinuclear analogues.[41] Exchange interactions in the excited state could not be determined, but previous studies found that the emissive $^2T_1{}^4A_2/^2E^4A_2$ states contain dinuclear spin states S of 1 and 2.[26a,41] Notably, the emission energy of Cr_2-PF_6 is higher than $[Cr(dNinp)_2]^{3+}$ (Figure 5c) by 750 cm^{-1}, which suggests that the degree of metal-ligand bond covalence in the dimer complex is lower than in the monomer complex, implying a larger Racah B parameter in the dinuclear complex.[2g,j,42] Thus, it seems that the charge-neutral pyridine ligands of dNinp form more covalent bonds than the anionic O-donor ligands in the dimer complex, leading to a weaker nephelauxetic effect in Cr_2-PF_6 than in $[Cr(dNinp)_2]^{3+}$.[42c,43]

The room temperature photoluminescence quantum yield Φ_{PL} of $[Cr(dNinp)_2](OTf)_3$ in deaerated acetonitrile is 0.03% (SI, section 6). The $^2T_1/^2E$ luminescence of $[Cr(dNinp)_2](OTf)_3$ decays with a luminescence lifetime τ_{PL} of 856 ± 13 ns in acetonitrile at room temperature and is essentially unaffected by oxygen from air (inset of Figure 6b, SI, Figure S7). These Φ_{PL} and τ_{PL} values are low compared to other recently investigated mononuclear Cr^{III} polypyridines.[2a–d,g,i] The $[Cr(dNinp)_2]^{3+}$ complex is tetragonally distorted already in the electronic ground state (Figure 3, Table 1), and it seems plausible that this can facilitate non-radiative relaxation from the $^2T_1/^2E$ excited states. Similar behavior has been observed for $[Ru(dNinp)_2]^{2+}$, which also features a tetragonally elongated octahedral coordination environment and which is non-luminescent in solution at room temperature.[29b] Back-intersystem crossing from the emissive $^2T_1/^2E$ states to the $^4T_2$ state in $[Cr(dNinp)_2]^{3+}$ seems difficult, due to the large ligand-field splitting. For the energetically high-lying $^2T_2$ and $^4T_1$ states, back- and forth intersystem crossing can in principle occur according to quantum chemical calculations performed for other Cr^{III} complexes.[44] Transient UV-vis absorption spectra of $[Cr(dNinp)_2](OTf)_3$ in aerated acetonitrile feature two negative signals centered at 355 nm and 425 nm (Figure 6a), corresponding to the bleach of the LMCT and mixed MC/LMCT absorption bands at these wavelengths (Figure 5a). The transient absorption band centered at 520 nm is attributed to the typical excited state absorption of the $^2T_1/^2E$ states.[12c,45] This band decays with a lifetime 868 ± 13 ns (Figure 6b), matching the abovementioned luminescence lifetimes and showing no detectable response to oxygen from air.

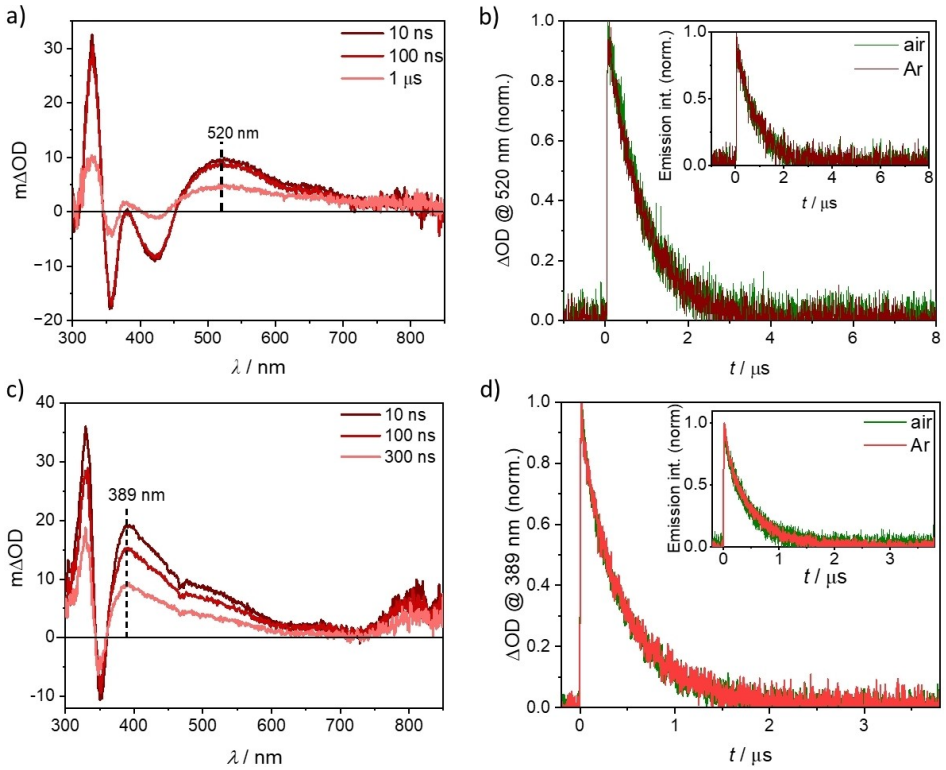

Figure 6. Transient absorption spectra of a) $[Cr(dNinp)_2](OTf)_3$ (50 µM) and c) Cr_2-PF_6 (80 µM) in aerated acetonitrile at 20 °C recorded with different time delays. b) Normalized decays of the transient absorption signal of $[Cr(dNinp)_2](OTf)_3$ at 520 nm recorded from a) together with the normalized luminescence decay at 774 nm (inset), both in aerated and deaerated acetonitrile at 20 °C. d) Normalized decays of the transient absorption signal of Cr_2-PF_6 at 389 nm from c) together with the normalized luminescence decay at 728 nm (inset), both in aerated and deaerated acetonitrile at 20 °C. Excitation occurred with a ns-pulsed laser at 425 nm (pulse energy of ~8 mJ, pulse duration ~10 ns) for $[Cr(dNinp)_2](OTf)_3$ and at 355 nm (pulse energy of ~40 mJ, pulse duration ~10 ns) for Cr_2-PF_6.

The luminescence of Cr^{III} polypyridine complexes is usually very sensitive to oxygen, mostly because the $^2T_1/^2E$ excited states are very long-lived with τ_{PL} from tens of microseconds to milliseconds.[2a–g,i,l,9a] The actual rate constants k_q for quenching of Cr^{III} spin-flip excited states by oxygen are typically only on the order of $10^7\ M^{-1}\,s^{-1}$ in solution at room temperature,[2a,g,20,46] far lower than for Ru^{II} complexes with luminescent ^{3}MLCT excited states.[17] The roughly 100-fold lower k_q values for Cr^{III} complexes are possibly related to the metal-centered character of their emissive spin-flip excited states, which are more shielded from the chemical environment (including dissolved O_2) than the ^{3}MLCT excited states of Ru^{II} polypyridine complexes.[2a,9e,20] However, the micro- to millisecond $^2T_1/^2E$ lifetimes of Cr^{III} polypyridines are between 1 and 3 orders of magnitude longer than the typical ^{3}MLCT lifetimes of Ru^{II} polypyridines, and this is the cause for the oxygen-sensitivity of Cr^{III} polypyridine luminescence despite relatively low quenching rate constants. Assuming that the rate constant for oxygen quenching k_q for $[Cr(dNinp)_2]^{3+}$ equals $10^7\ M^{-1}\,s^{-1}$, and given the oxygen solubility of ~2.4 mM in aerated acetonitrile at room temperature,[47] the expectable rate for pseudo first order bimolecular reaction of $^2T_1/^2E$-excited $[Cr(dNinp)_2]^{3+}$ with O_2 is $10^7\ M^{-1}\,s^{-1}\times 2.4\cdot10^{-3}\ M = 2.4\cdot10^4\ s^{-1}$. The inherent $^2T_1/^2E$ decay rate according to the luminescence and transient absorption experiments reported above is $(860\ ns)^{-1} = 1.16\cdot10^6\ s^{-1}$, and thus the expectable luminescence lifetime quenching by oxygen from air amounts to only a factor of $2.4\cdot10^4\ s^{-1}/1.16\cdot10^6\ s^{-1} = 0.02$, which falls within the detection limits of the respective experiments. This analysis leads to the conclusion that the comparatively short luminescence lifetime (860 ns) of $[Cr(dNinp)_2]^{3+}$, together with the comparatively low rate constants expectable for bimolecular quenching of Cr^{III} spin-flip excited states by O_2,[2a–g,i,l,9a] can account for the unusual insensitivity of their photoluminescence to oxygen from air.

For the dinuclear $[Cr_2dNinp_2(\mu\text{-}OH)_2(\mu\text{-}O_2CMe)]^{3+}$ complex, the photoluminescence quantum yield Φ_{PL} is ~0.01% in aerated acetonitrile at room temperature, with a luminescence lifetime of 449 ± 3 ns for Cr_2-PF_6 and 457 ± 7 ns for Cr_2-OTf (inset of Figure 6d, Figures S11/S12). This Φ_{PL} value is a factor of 3 lower than for $[Cr(dNinp)_2]^{3+}$ and the lifetime is a factor of ~2 shorter, indicating more efficient non-radiative excited-state relaxation in the dimer compared to the mononuclear complex. This finding could be due to the more distorted octahedral geometry in the ground- and excited states in the dimer, and perhaps also because the hydroxo and acetato bridging units are particularly efficient in dissipating the excitation energy into molecular vibrations. The $^2T_1{}^4A_2/^2E^4A_2$ energy of the dinuclear Cr^{III} complex (~13700 cm^{-1}) corresponds fairly well to the third overtone ($\nu = 4$) of the typical OH vibrational energy (~3400 cm^{-1}),[48] which can lead to multiphonon relaxations due to the bridging OH groups.[2b,c,g,42d] Transient UV-vis absorption spectra show a bleach at 350 nm, reflecting the disappearance of the LMCT ground-state absorption, and a band peaking at 389 nm with a shoulder ~500 nm (Figure 6c), reflecting excited state absorptions. Kinetic measurement of the transient absorption signal at 389 nm gives a time constant that is essentially identical to the luminescence lifetimes, and all of these decays are oxygen-independent for the same reason as explained above for the mononuclear complex (Figure 6d, Figures S13/S14).

Energy Transfer and Upconversion

The $^2T_1/^2E$ excited states of Cr^{III} emitters can undergo doublet-doublet energy transfer (self-exchange reactions)[49] and doublet-triplet energy transfer (DTET) processes,[11b] which are spin-allowed as long as the total spin of the donor-acceptor pair is conserved.[50] Doublet-triplet energy transfer from a previously investigated mononuclear Cr^{III} polypyridine complex to anthracene molecules has been found to approach nearly unit efficiency, and the $^2E/^2T_1$ excited-state quenching rate constant k_{DTET} reached values that were more than one order of magnitude above the typical k_q values for $^2T_1/^2E$ excited state quenching by oxygen ($10^7\ M^{-1}\,s^{-1}$, see above).[2g,11b] Nonetheless, quenching by oxygen can remain a competitive unwanted reaction pathway, given the very long $^2T_1/^2E$ lifetimes of many recently reported Cr^{III} polypyridines. The oxygen insensitive excited-state behavior of our new mono- and dinuclear Cr^{III} emitters seems attractive for DTET to organic chromophores, because O_2 is an uncompetitive quencher, which could permit energy transfer under aerobic conditions without forming aggressive $^1O_2$ species that induce unwanted photo-degradation. However, the possibility of undesirable reactions between O_2 and a long-lived triplet excited state of the energy acceptor remains in this scenario.

9,10-bis((triisopropylsilyl)ethynyl)anthracene ($AnTIPS_2$) is a well-known blue-emissive fluorophore that is frequently used in sensitized triplet-triplet annihilation upconversion (sTTA-UC) systems.[11a,51] The lowest triplet (T_1) excited state of $AnTIPS_2$ (~1.39–1.55 eV)[51d] is energetically below the emissive $^2T_1{}^4A_2/^2E^4A_2$ excited states of the dinuclear $[Cr_2dNinp_2(\mu\text{-}OH)_2(\mu\text{-}O_2CMe)]^{3+}$ (1.70 eV), and hence an exergonic DTET is expected. Stern-Volmer study shows a luminescence lifetime quenching by $AnTIPS_2$ with a rate constant k_{DTET} of $1.63\times10^9\ M^{-1}\,s^{-1}$ in deaerated acetonitrile/toluene (1:1) at 20 °C (Figure 7a, SI, section 7), which is below the diffusion limit of the employed solvents ($k_{diff} > 1.0\times10^{10}\ M^{-1}\,s^{-1}$).[52] The k_{DTET} value determined here is more than 25 fold higher than that found for a mononuclear Cr^{III} polypyridine and anthracenes in *N*, *N*-dimethylformamide ($(5.6–6.4)\times10^7\ M^{-1}\,s^{-1}$).[11b] This is likely attributable to the larger driving force for DTET from our Cr^{III} dimer to $AnTIPS_2$ (−(0.15–0.31) eV) in comparison to the previously investigated system comprised of a mononuclear Cr^{III} complex to anthracenes (> −0.03 eV).[50]

Selective photoexcitation of Cr_2-OTf at 532 nm in the presence of 2.3 mM $AnTIPS_2$ leads to a blue emission from the singlet state of $AnTIPS_2$ centered at 470 nm and a red phosphorescence from the $^2T_1{}^4A_2/^2E^4A_2$ states of Cr_2-OTf. Whilst the prompt $^2T_1{}^4A_2/^2E^4A_2$ phosphorescence of Cr_2-OTf is only observable at comparatively short delays after laser excitation (red trace in Figure 7b), the blue $AnTIPS_2$ emission remains detectable after a delay time of 50 μs (blue trace in Figure 7b). The upconversion emission intensity at 470 nm decays with a lifetime of 222 μs (Figure 7b, inset), exceeding the prompt fluorescence lifetime of $AnTIPS_2$ (5.2 ns) more than 40000

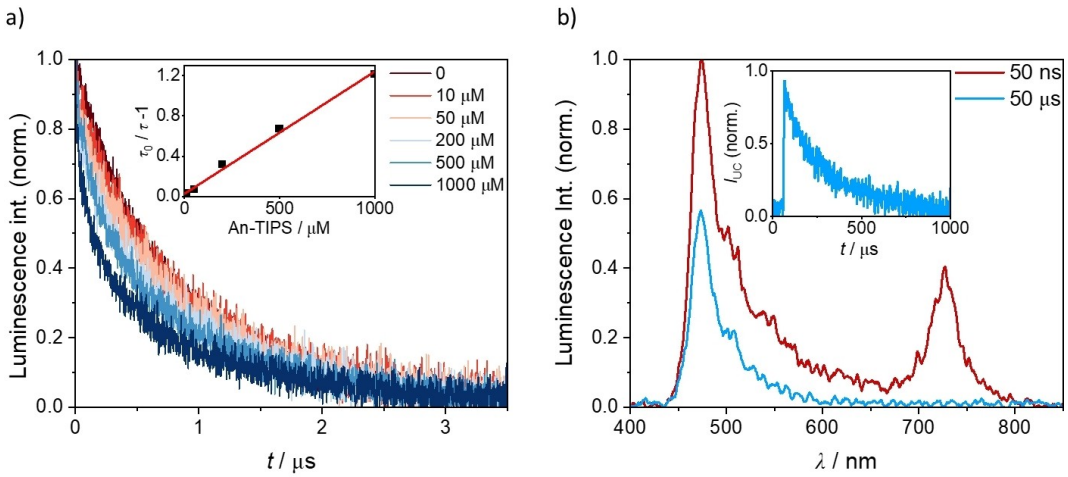

Figure 7. a) Stern-Volmer study of **Cr_2-OTf** (150 μM) in deaerated acetonitrile/toluene (1 : 1) at 20 °C with An-$TIPS_2$: normalized luminescence decay of **Cr_2-OTf** at 728 nm with An-$TIPS_2$ of different concentrations under excitation with a ~10 ns pulsed 532 nm laser (pulse energy ~50 mJ). Mono-exponential fit of the decays yields the lifetimes τ for any given quencher concentration. Inset: Stern-Volmer plot based on lifetime quenching derived from the decays in the main plot. b) Luminescence spectra of **Cr_2-OTf** (100 μM) + An-$TIPS_2$ (2.3 mM) in deaerated acetonitrile/toluene (1 : 1) at 20 °C recorded with different time delays and the luminescence decay at 470 nm (inset). Excitation occurred with a ns-pulsed laser at 532 nm (pulse energy of ~50 mJ). Mono-exponential fit of the decay in the inset of b) gives an upconversion luminescence lifetime of 222 μs.

times,[11b] confirming the delayed nature of the upconverted luminescence that reflects the T_1 lifetime of $AnTIPS_2$.[11a] Collectively, the data set in Figure 7 demonstrates that luminescent dinuclear Cr^{III} complexes are amenable to energy transfer catalysis and photon upconversion.

Conclusions

Numerous recent works on photoactive coordination compounds including mononuclear Cr^{III} polypyridines and other first-row transition metal complexes concentrated on optimizing the octahedral coordination symmetry.[2a,c,d,g,3a,8a,53] Here, we used a tridentate chelate ligand that leads to tetragonally elongated primary coordination spheres around Cr^{III}, causing lifetimes of the luminescent spin-flip excited states that are considerably shorter than those of recently reported Cr^{III} polypyridines yet remain similarly long as the ^{3}MLCT lifetimes of Ru^{II} polypyridines and Cu^{I} diimines.[6e,21,54] Unlike these ^{3}MLCT emitters, the luminescent spin-flip excited states of our Cr^{III} complexes are insensitive to oxygen from air, presumably because the spin-flip excitation is electronically more decoupled from the chemical environment. This oxygen insensitivity paired with lifetimes in the hundreds of nanoseconds seems fundamentally attractive for Cr^{III} based photoredox catalysis, because it avoids the formation of $^1O_2$, which can interfere in Cr^{III} based photoredox cycles.[14,55] Cleaner and more predictable photochemistry could in principle result.

Many tridentate ligands explored recently for photoactive metal complexes lead to either meridional or facial coordination modes, whereas the ligand used herein is sufficiently flexible to allow for both meridional and facial coordination. This in turn enabled the synthesis of either a mononuclear or a dinuclear Cr^{III} complex depending on well-controllable reaction conditions. The obtained Cr^{III} dimer features ferromagnetic exchange interactions in the electronic ground state, and its luminescent excited state undergoes energy transfer and photon upconversion with an anthracene derivative under green light excitation.

So far, dinuclear Cr^{III} complexes have been mostly explored with regard to their magnetic properties, while their photoluminescence behavior has received very limited attention and often was restricted to cryogenic temperatures.[23,28,41] This can be likely attributed to the comparatively weak ligand fields established in such Cr^{III} dimers until now, leading to rapid energy dissipation by efficient back intersystem crossing from the luminescent spin-flip excited states into higher-lying non-radiatively deactivating excited states.[26a] Our study reveals new guidelines for controlled synthetic access to luminescent dinuclear Cr^{III} complexes with ferromagnetic coupling and sufficiently strong ligand fields for room temperature luminescence. These insights could open the door to fundamentally new discoveries at the interface of molecular magnetism, photophysics, and photochemistry.[56]

Crystallographic Data

Deposition Number(s) 2342690 (for $[Cr(dNinp)_2]^{3+}$), 2342691 (for PF_6-salt of Cr(III) dimer), 2342692 (for OTf-salt of Cr(III) dimer) contain(s) the supplementary crystallographic data for this paper. These data are provided free of charge by the joint Cambridge Crystallographic Data Centre and Fachinformationszentrum Karlsruhe Access Structures service.

Acknowledgements

O. S. W. acknowledges funding from the Swiss National Science Foundation through grant number 200020_207329 and from

the Swiss Nanoscience Institute (SNI) through project P1908. C. W. thanks the Deutsche Forschungsgemeinschaft (DFG, German Research Foundation) for the grant with project number 535142873, and F. M. thanks the DFG for the grant with the project number 404391096 in the framework of the SPP 2102. Purchase of the SQUID magnetometer was enabled by the DFG (project number 423442764; INST 186/1329-1 FUGG) and the Niedersächsische Ministerium für Wissenschaft und Kultur (MWK). Open Access funding enabled and organized by Projekt DEAL.

Conflict of Interests

The authors declare no conflict of interest.

Data Availability Statement

The data that support the findings of this study are openly available in Zenodo at https://doi.org/10.5281/zenodo.10728245, reference number 10728245.

Keywords: chromium(III) complexes · ferromagnetic coupling · photoluminescence · laser spectroscopy · sensitized triplet-triplet annihilation upconversion

[1] a) M. Dorn, J. Kalmbach, P. Boden, A. Papcke, S. Gomez, C. Förster, F. Kuczelinis, L. M. Carrella, L. A. Büldt, N. H. Bings, E. Rentschler, S. Lochbrunner, L. Gonzalez, M. Gerhards, M. Seitz, K. Heinze, *J. Am. Chem. Soc.* **2020**, *142*, 7947–7955; b) M. Dorn, J. Kalmbach, P. Boden, A. Kruse, C. Dab, C. Reber, G. Niedner-Schatteburg, S. Lochbrunner, M. Gerhards, M. Seitz, K. Heinze, *Chem. Sci.* **2021**, *12*, 10780–10790; c) J. P. Zobel, T. Knoll, L. González, *Chem. Sci.* **2021**, *12*, 10791–10801.

[2] a) S. Otto, M. Grabolle, C. Förster, C. Kreitner, U. Resch-Genger, K. Heinze, *Angew. Chem. Int. Ed.* **2015**, *54*, 11572–11576; b) C. Wang, S. Otto, M. Dorn, E. Kreidt, J. Lebon, L. Srsan, P. Di Martino-Fumo, M. Gerhards, U. Resch-Genger, M. Seitz, K. Heinze, *Angew. Chem. Int. Ed.* **2018**, *57*, 1112–1116; c) S. Treiling, C. Wang, C. Förster, F. Reichenauer, J. Kalmbach, P. Boden, J. P. Harris, L. M. Carrella, E. Rentschler, U. Resch-Genger, C. Reber, M. Seitz, M. Gerhards, K. Heinze, *Angew. Chem. Int. Ed.* **2019**, *58*, 18075–18085; d) J. R. Jiménez, B. Doistau, C. M. Cruz, C. Besnard, J. M. Cuerva, A. G. Campaña, C. Piguet, *J. Am. Chem. Soc.* **2019**, *141*, 13244–13252; e) R. Farran, L. Le-Quang, J. M. Mouesca, V. Maurel, D. Jouvenot, F. Loiseau, A. Deronzier, J. Chauvin, *Dalton Trans.* **2019**, *48*, 6800–6811; f) J.-R. Jiménez, B. Doistau, M. Poncet, C. Piguet, *Coord. Chem. Rev.* **2021**, *434*, 213750; g) F. Reichenauer, C. Wang, C. Förster, P. Boden, N. Ugur, R. Báez-Cruz, J. Kalmbach, L. M. Carrella, E. Rentschler, C. Ramanan, G. Niedner-Schatteburg, M. Gerhards, M. Seitz, U. Resch-Genger, K. Heinze, *J. Am. Chem. Soc.* **2021**, *143*, 11843–11855; h) C. Wegeberg, D. Häussinger, O. S. Wenger, *J. Am. Chem. Soc.* **2021**, *143*, 15800–15811; i) J. R. Jiménez, M. Poncet, S. Miguez-Lago, S. Grass, J. Lacour, C. Besnard, J. M. Cuerva, A. G. Campaña, C. Piguet, *Angew. Chem. Int. Ed.* **2021**, *60*, 10095–10102; j) N. Sinha, J. R. Jimenez, B. Pfund, A. Prescimone, C. Piguet, O. S. Wenger, *Angew. Chem. Int. Ed.* **2021**, *60*, 23722–23728; k) N. Sinha, C. Wegeberg, D. Häussinger, A. Prescimone, O. S. Wenger, *Nat. Chem.* **2023**, *15*, 1730–1736; l) R. W. Jones, A. J. Auty, G. Wu, P. Persson, M. V. Appleby, D. Chekulaev, C. R. Rice, J. A. Weinstein, P. I. P. Elliott, P. A. Scattergood, *J. Am. Chem. Soc.* **2023**, *145*, 12081–12092; m) C. Wegeberg, D. Häussinger, S. Kupfer, O. S. Wenger, *J. Am. Chem. Soc.* **2024**, *146*, 4605–4619, 10.1021/jacs.1023c11580.

[3] a) P. Herr, C. Kerzig, C. B. Larsen, D. Häussinger, O. S. Wenger, *Nat. Chem.* **2021**, *13*, 956–962; b) N. R. East, R. Naumann, C. Förster, C. Ramanan, G. Diezemann, K. Heinze, *Nat. Chem.* **2024**, 10.1038/s41557-41024-01446-41558; c) M. Scaccaglia, M. P. Birbaumer, S. Pinelli, G. Pelosi, A. Frei, *Chem. Sci.* **2024**, *15*, 3907–3919, DOI: 10.1039/d1033sc05326a.

[4] a) K. S. Kjær, N. Kaul, O. Prakash, P. Chábera, N. W. Rosemann, A. Honarfar, O. Gordivska, L. A. Fredin, K.-E. Bergquist, L. Häggström, T. Ericsson, L. Lindh, A. Yartsev, S. Styring, P. Huang, J. Uhlig, J. Bendix, D. Strand, V. Sundström, P. Persson, R. Lomoth, K. Wärnmark, *Science* **2019**, *363*, 249–253; b) J. Steube, A. Kruse, O. S. Bokareva, T. Reuter, S. Demeshko, R. Schoch, M. A. Arguello Cordero, A. Krishna, S. Hohloch, F. Meyer, K. Heinze, O. Kühn, S. Lochbrunner, M. Bauer, *Nat. Chem.* **2023**, *15*, 468–474; c) Y. Ye, P. Garrido-Barros, J. Wellauer, C. M. Cruz, R. Lescouëzec, O. S. Wenger, J. M. Herrera, J. R. Jiménez, *J. Am. Chem. Soc.* **2024**, *146*, 954–960.

[5] a) T. Eskelinen, S. Buss, S. K. Petrovskii, E. V. Grachova, M. Krause, L. Kletsch, A. Klein, C. A. Strassert, I. O. Koshevoy, P. Hirva, *Inorg. Chem.* **2021**, *60*, 8777–8789; b) S. I. Ting, S. Garakyaraghi, C. M. Taliaferro, B. J. Shields, G. D. Scholes, F. N. Castellano, A. G. Doyle, *J. Am. Chem. Soc.* **2020**, *142*, 5800–5810; c) T. Ogawa, O. S. Wenger, *Angew. Chem. Int. Ed.* **2023**, *62*, e202312851; d) T. Ogawa, N. Sinha, B. Pfund, A. Prescimone, O. S. Wenger, *J. Am. Chem. Soc.* **2022**, *144*, 21948–21960.

[6] a) A. Hossain, A. Bhattacharyya, O. Reiser, *Science* **2019**, *364*; b) M. Gernert, L. Balles-Wolf, F. Kerner, U. Muller, A. Schmiedel, M. Holzapfel, C. M. Marian, J. Pflaum, C. Lambert, A. Steffen, *J. Am. Chem. Soc.* **2020**, *142*, 8897–8909; c) R. Hamze, J. L. Peltier, D. Sylvinson, M. Jung, J. Cardenas, R. Haiges, M. Soleilhavoup, R. Jazzar, P. I. Djurovich, G. Bertrand, M. E. Thompson, *Science* **2019**, *363*, 601–606; d) T. Brandl, C. Kerzig, L. Le Pleux, A. Prescimone, O. S. Wenger, M. Mayor, *Chem. Eur. J.* **2020**, *26*, 3119–3128; e) J. Beaudelot, S. Oger, S. Peruško, T. A. Phan, T. Teunens, C. Moucheron, G. Evano, *Chem. Rev.* **2022**, *122*, 16365–16609; f) F. Doettinger, Y. Yang, M. Karnahl, S. Tschierlei, *Inorg. Chem.* **2023**, *62*, 8166–8178; g) M. Rentschler, P. J. Boden, M. A. Arguello Cordero, S. T. Steiger, M. A. Schmid, Y. Yang, G. Niedner-Schatteburg, M. Karnahl, S. Lochbrunner, S. Tschierlei, *Inorg. Chem.* **2022**, *61*, 12249–12261.

[7] a) R. Tabone, D. Feser, E. D. Lemma, U. Schepers, C. Bizzarri, *Front. Chem.* **2021**, *9*, 754420; b) J. A. Kübler, B. Pfund, O. S. Wenger, *JACS Au* **2022**, *2*, 2367–2380; c) O. Mrózek, M. Mitra, B. Hupp, A. Belyaev, N. Lüdtke, D. Wagner, C. Wang, O. S. Wenger, C. M. Marian, A. Steffen, *Chem. Eur. J.* **2023**, *29*, e202203980.

[8] a) N. Sinha, O. S. Wenger, *J. Am. Chem. Soc.* **2023**, *145*, 4903–4920; b) C. Wegeberg, O. S. Wenger, *JACS Au* **2021**, *1*, 1860–1876; c) C. Förster, K. Heinze, *Chem. Soc. Rev.* **2020**, *49*, 1057–1070; d) C. Förster, K. Heinze, *Chem. Phys. Rev.* **2022**, *3*, 041302; e) W. R. Kitzmann, J. Moll, K. Heinze, *Photochem. Photobiol. Sci.* **2022**, *21*, 1309–1331.

[9] a) C. Wang, S. Otto, M. Dorn, K. Heinze, U. Resch-Genger, *Anal. Chem.* **2019**, *91*, 2337–2344; b) S. Otto, J. P. Harris, K. Heinze, C. Reber, *Angew. Chem. Int. Ed.* **2018**, *57*, 11069–11073; c) S. Otto, N. Scholz, T. Behnke, U. Resch-Genger, K. Heinze, *Chem. Eur. J.* **2017**, *23*, 12131–12135; d) I. Strelnik, A. Shamsieva, K. Akhmadgaleev, T. Gerasimova, I. Dayanova, I. Kolesnikov, R. Fayzullin, D. Islamov, E. Musina, A. Karasik, O. Sinyashin, *Chem. Eur. J.* **2023**, *29*, e202202864; e) C. Wang, W. R. Kitzmann, F. Weigert, C. Förster, X. Wang, K. Heinze, U. Resch-Genger, *ChemPhotoChem* **2022**, *6*, e202100296.

[10] L. P. Ravaro, K. P. S. Zanoni, A. S. S. de Camargo, *Energy Rep.* **2020**, *6*, 37–45.

[11] a) C. Wang, C. Wegeberg, O. S. Wenger, *Angew. Chem. Int. Ed.* **2023**, *61*, e202311470; b) C. Wang, F. Reichenauer, W. R. Kitzmann, C. Kerzig, K. Heinze, U. Resch-Genger, *Angew. Chem. Int. Ed.* **2022**, *61*, e202202238; c) F. Glaser, O. S. Wenger, *JACS Au* **2022**, *2*, 1488–1503; d) K. M. Felter, M. C. Fravventura, E. Koster, R. D. Abellon, T. J. Savenije, F. C. Grozema, *ACS Energy Lett.* **2020**, *5*, 124–129; e) Z. Mahmood, N. Rehmat, S. Ji, J. Zhao, S. Sun, M. Di Donato, M. Li, M. Teddei, Y. Huo, *Chemistry* **2020**, *26*, 14912–14918; f) J. Kalmbach, C. Wang, Y. You, C. Forster, H. Schubert, K. Heinze, U. Resch-Genger, M. Seitz, *Angew. Chem. Int. Ed.* **2020**, *59*, 18804–18808.

[12] a) B. M. Hockin, C. Li, N. Robertson, E. Zysman-Colman, *Catal. Sci. Technol.* **2019**, *9*, 889–915; b) P. A. Scattergood in *Recent advances in chromium coordination chemistry: luminescent materials and photocatalysis*, Royal Society of Chemistry, Cambridge, **2020**, *43*, pp. 1–34; c) T. H. Bürgin, F. Glaser, O. S. Wenger, *J. Am. Chem. Soc.* **2022**, *144*, 14181–14194; d) W. R. Kitzmann, K. Heinze, *Angew. Chem. Int. Ed.* **2022**, *62*, e202213207; e) S. Sittel, R. Naumann, K. Heinze, *Front. Chem.* **2022**, *10*, 887439; f) M. D. Woodhouse, J. K. McCusker, *J. Am. Chem. Soc.* **2020**, *142*, 16229–16233; g) A. Aydogan, R. E. Bangle, A. Cadranel, M. D. Turlington, D. T. Conroy, E. Cauët, M. L. Singleton, G. J. Meyer, R. N. Sampaio, B. Elias, L. Troian-Gautier, *J. Am. Chem. Soc.* **2021**, *143*, 15661–15673; h) L. H. M. de Groot, A. Ilic, J. Schwarz, K. Wärnmark, *J. Am. Chem.*

Soc. **2023**, *145*, 9369–9388; i) C. Minozzi, A. Caron, J. C. Grenier-Petel, J. Santandrea, S. K. Collins, *Angew. Chem. Int. Ed.* **2018**, *57*, 5477–5481; j) Amy Y. Chan, Atanu Ghosh, Jonathan T. Yarranton, Jack Twilton, Jian Jin, Daniela M. Arias-Rotondo, Holt A. Sakai, James K. McCusker, D. W. C. MacMillan, *Science* **2023**, *382*, 191–197.
[13] S. Otto, M. Dorn, C. Förster, M. Bauer, M. Seitz, K. Heinze, *Coord. Chem. Rev.* **2018**, *359*, 102–111.
[14] S. Sittel, A. C. Sell, K. Hofman, C. Wiedemann, J. P. Nau, C. Kerzig, G. Manolikakes, K. Heinze, *ChemCatChem* **2023**, *15*, e202201562.
[15] a) F. A. Baptista, D. Krizsan, M. Stitch, I. V. Sazanovich, I. P. Clark, M. Towrie, C. Long, L. Martinez-Fernandez, R. Improta, N. A. P. Kane-Maguire, J. M. Kelly, S. J. Quinn, *J. Am. Chem. Soc.* **2021**, *143*, 14766–14779; b) C. Wang, K. Ebel, K. Heinze, U. Resch-Genger, I. Bald, *Chem. Eur. J.* **2023**, *29*, e202203719.
[16] D. L. Dexter, *J. Chem. Phys.* **1953**, *21*, 836–850.
[17] A. A. Abdel-Shafi, M. D. Ward, R. Schmidt, *Dalton Trans.* **2007**, 2517–2527.
[18] S. Otto, A. M. Nauth, E. Ermilov, N. Scholz, A. Friedrich, U. Resch-Genger, S. Lochbrunner, T. Opatz, K. Heinze, *ChemPhotoChem* **2017**, *1*, 344–349.
[19] U. Basu, S. Otto, K. Heinze, G. Gasser, *Eur. J. Inorg. Chem.* **2018**, *2019*, 37–41.
[20] L. Stein, C. Wang, C. Förster, U. Resch-Genger, K. Heinze, *Dalton Trans.* **2022**, *51*, 17664–17670.
[21] D. M. Arias-Rotondo, J. K. McCusker, *Chem. Soc. Rev.* **2016**, *45*, 5803–5820.
[22] A. Døssing, *Coord. Chem. Rev.* **2014**, *280*, 38–53.
[23] a) J. Ferguson, H. U. Güdel, *Aust. J. Chem.* **1973**, *26*, 505–511; b) Silvio Decurtins, Hans U. Güdel, A. Pfeuti, *Inorg. Chem.* **1982**, *21*, 1101–1106; c) Silvio Decurtins, H. U. Güdel, *Inorg. Chem.* **1982**, *21*, 3598–3606.
[24] a) J.-H. Jia, Q.-W. Li, Y.-C. Chen, J.-L. Liu, M.-L. Tong, *Coord. Chem. Rev.* **2019**, *378*, 365–381; b) S. Zanella, M. Aragon-Alberti, C. D. S. Brite, F. Salles, L. D. Carlos, J. Long, *Angew. Chem. Int. Ed.* **2023**, *62*, e202306970.
[25] a) T. J. Morsing, J. Bendix, H. Weihe, A. Døssing, *Inorg. Chem.* **2014**, *53*, 2996–3003; b) H. W. L. Fraser, G. S. Nichol, G. Velmurugan, G. Rajaraman, E. K. Brechin, *Dalton Trans.* **2017**, *46*, 7159–7168.
[26] a) Christian Reber, Hans U. Güdel, Leone Spiccia, W. Marty, *Inorg. Chem.* **1987**, *26*, 3186–3191; b) Ralf Sanzenbacher, Arnd Böttcher, Horst Elias, Martina Hüber, Wolfgang Haase, Jørgen Glerup, Thomas B. Jensen, Markus Neuburger, Margareta Zehnder, Johan Springborg, C. E. Olsen, *Inorg. Chem.* **1996**, *35*, 7493–7499; c) T. J. Morsing, H. Weihe, J. Bendix, *Eur. J. Inorg. Chem.* **2014**, *2014*, 5990–5996; d) J. Rinck, J. A. Kitchen, A. B. Carter, Y. Lan, C. E. Anson, K. Fink, S. Brooker, A. K. Powell, *Front. Chem.* **2020**, *8*, 540.
[27] H. W. L. Fraser, L. Smythe, S. Dey, G. S. Nichol, S. Piligkos, G. Rajaraman, E. K. Brechin, *Dalton Trans.* **2018**, *47*, 8100–8109.
[28] M. Börner, J. Klose, M. E. Gutierrez Suburu, C. A. Strassert, F. Yang, K. Y. Monakhov, B. Abel, B. Kersting, *Chem. Eur. J.* **2021**, *27*, 14899–14910.
[29] a) M. Abrahamsson, M. Jäger, T. Österman, L. Eriksson, P. Persson, H. C. Becker, O. Johansson, L. Hammarström, *J. Am. Chem. Soc.* **2006**, *128*, 12616–12617; b) G. A. Parada, L. A. Fredin, M. P. Santoni, M. Jäger, R. Lomoth, L. Hammarström, O. Johansson, P. Persson, S. Ott, *Inorg. Chem.* **2013**, *52*, 5128–5137; c) A. Breivogel, C. Förster, K. Heinze, *Inorg. Chem.* **2010**, *49*, 7052–7056.
[30] K. L. Garner, L. F. Parkes, J. D. Piper, J. A. Williams, *Inorg. Chem.* **2010**, *49*, 476–487.
[31] a) J. R. Jiménez, B. Doistau, C. Besnard, C. Piguet, *Chem. Commun.* **2018**, *54*, 13228–13231; b) J. Chong, C. Besnard, C. M. Cruz, C. Piguet, J. R. Jiménez, *Dalton Trans.* **2022**, *51*, 4297–4309; c) D. Zare, B. Doistau, H. Nozary, C. Besnard, L. Guénée, Y. Suffren, A. L. Pelé, A. Hauser, C. Piguet, *Dalton Trans.* **2017**, *46*, 8992–9009.
[32] a) Kazuhiko Yamada, Shuan Dong, G. Wu, *J. Am. Chem. Soc.* **2000**, *122*, 11602–11609; b) B. Srinivasa Rao, A. Srivani, D. Dhana Lakshmi, N. Lingaiah, *Catal. Lett.* **2016**, *146*, 2025–2031.
[33] R. H. Duncan Lyngdoh, H. F. Schaefer III, R. B. King, *Chem. Rev.* **2018**, *118*, 11626–11706.
[34] K. Tono, A. Terasaki, T. Ohta, T. Kondow, *Phys. Rev. Lett.* **2003**, *90*, 133402.
[35] J. Springborg, *Adv. Inorg. Chem.* **1988**, *32*, 55–169.
[36] H. Xiang, J. Cheng, X. Ma, X. Zhou, J. J. Chruma, *Chem. Soc. Rev.* **2013**, *42*, 6128–6185.
[37] a) N. Serpone, M. A. Jamieson, M. S. Henry, M. Z. Hoffman, F. Bolletta, M. Maestri, *J. Am. Chem. Soc.* **1979**, *101*, 2907–2916; b) J. C. Barbour, A. J. I. Kim, E. deVries, S. E. Shaner, B. M. Lovaasen, *Inorg. Chem.* **2017**, *56*, 8212–8222; c) B. Doistau, J. R. Jiménez, L. M. Lawson Daku, C. Piguet, *Inorg. Chem.* **2022**, *61*, 11023–11031.
[38] T. Brandl, V. Hoffmann, A. Pannwitz, D. Häussinger, M. Neuburger, O. Fuhr, S. Bernhard, O. S. Wenger, M. Mayor, *Chem. Sci.* **2018**, *9*, 3837–3843.
[39] L. S. Forster, *Chem. Rev.* **1990**, *90*, 331–353.
[40] a) H. Riesen, H. U. Güdel, *Mol. Phys.* **1987**, *60*, 1221–1244; b) P. J. McCarthy, H. U. Güdel, *Coord. Chem. Rev.* **1988**, *88*, 69–131.
[41] R. Schenker, H. Weihe, H. U. Güdel, B. Kersting, *Inorg. Chem.* **2001**, *40*, 3355–3362.
[42] a) L. Stein, P. Boden, R. Naumann, C. Förster, G. Niedner-Schatteburg, K. Heinze, *Chem. Commun.* **2022**, *58*, 3701–3704; b) N. Sawicka, C. J. Craze, P. N. Horton, S. J. Coles, E. Richards, S. J. A. Pope, *Chem. Commun.* **2022**, *58*, 5733–5736; c) N. Sinha, P. Yaltseva, O. S. Wenger, *Angew. Chem. Int. Ed.* **2023**, *62*, e202303864; d) Y. Cheng, Q. Yang, J. He, W. Zou, K. Liao, X. Chang, C. Zou, W. Lu, *Dalton Trans.* **2023**, *52*, 2561–2565.
[43] C. E. Housecroft, A. G. Sharpe, *Inorganic Chemistry*, 4th edition, Pearson, Essex, **2012**, p 698.
[44] J. P. Zobel, H. Radatz, L. González, *Molecules* **2023**, *28*, 1668.
[45] W. R. Kitzmann, C. Ramanan, R. Naumann, K. Heinze, *Dalton Trans.* **2022**, *51*, 6519–6525.
[46] a) A. Pfeil, *J. Am. Chem. Soc.* **1971**, *93*, 5395–5398 ; b) B. Brunschwig, N. Sutin, *J. Am. Chem. Soc.* **1978**, *100*, 7568–7577; c) A. M. M. Alazaly, G. J. Clarkson, M. D. Ward, A. A. Abdel-Shafi, *Inorg. Chem.* **2023**, *62*, 16101–16113.
[47] C. Franco, J. Olmsted III, *Talanta* **1990**, *37*, 905–909.
[48] R. L. Swofford, M. E. Long, M. S. Burberry, A. C. Albrecht, *J. Chem. Phys.* **1977**, *66*, 664–668.
[49] a) M. T. Vagnini, W. C. Rutledge, P. S. Wagenknecht, *Inorg. Chem.* **2010**, *49*, 833–838; b) P. S. Wagenknecht, N. A. P. Kane-Maguire, D. G. Speece, N. Helwic, *Inorg. Chem.* **2002**, *41*, 1229–1235.
[50] D. Guo, T. E. Knight, J. K. McCusker, *Science* **2011**, *334*, 1684–1687.
[51] a) H. Tamura, *J. Phys. Chem. A* **2020**, *124*, 7943–7949; b) J. K. Li, M. Y. Zhang, L. Zeng, L. Huang, X. Y. Wang, *Angew. Chem. Int. Ed.* **2023**, *62*, e202303093; c) S. N. Sanders, T. H. Schloemer, M. K. Gangishetty, D. Anderson, M. Seitz, A. O. Gallegos, R. C. Stokes, D. N. Congreve, *Nature* **2022**, *604*, 474–478; d) N. Nishimura, V. Gray, J. R. Allardice, Z. Zhang, A. Pershin, D. Beljonne, A. Rao, *ACS Materials Lett.* **2019**, *1*, 660–664.
[52] a) M. Montalti, A. Credi, L. Prodi, M. T. Gandolfi, *Handbook of Photochemistry*, CRC Press, Boca Raton, **2006**, p. 424; b) T. W. Schmidt, F. N. Castellano, *J. Phys. Chem. Lett.* **2014**, *5*, 4062–4072.
[53] a) L. L. Jamula, A. M. Brown, D. Guo, J. K. McCusker, *Inorg. Chem.* **2014**, *53*, 15–17; b) M. Darari, A. Francés-Monerris, B. Marekha, A. Doudouh, E. Wenger, A. Monari, S. Haacke, P. C. Gros, *Molecules* **2020**, *25*, 5991; c) T. Reuter, A. Kruse, R. Schoch, S. Lochbrunner, M. Bauer, K. Heinze, *Chem. Commun.* **2021**, *57*, 7541–7544.
[54] S. Cerfontaine, L. Troian-Gautier, Q. Duez, J. Cornil, P. Gerbaux, B. Elias, *Inorg. Chem.* **2021**, *60*, 366–379.
[55] a) L. A. Büldt, O. S. Wenger, *Chem. Sci.* **2017**, *8*, 7359–7367; b) R. F. Higgins, S. M. Fatur, S. G. Shepard, S. M. Stevenson, D. J. Boston, E. M. Ferreira, N. H. Damrauer, A. K. Rappe, M. P. Shores, *J. Am. Chem. Soc.* **2016**, *138*, 5451–5464.
[56] T. J. Penfold, J. O. Johansson, J. Eng, *Coord. Chem. Rev.* **2023**, *494*, 215346.

Manuscript received: February 29, 2024
Accepted manuscript online: March 25, 2024
Version of record online: May 14, 2024